Results in Physics xxx (2017) xxx–xxx

Contents lists available at ScienceDirect

Results in Physics

journal homepage: www.journals.elsevier.com/results-in-physics

Study of the synergistic effect of 2-methoxy-4-formylphenol and sodium molybdenum oxide on the corrosion inhibition of 3CR12 ferritic steel in dilute sulphuric acid

Roland Tolulope Loto

Department of Mechanical Engineering, Covenant University, Ota, Ogun State, Nigeria

ARTICLE INFO

Article history:
Received 18 January 2017
Accepted 31 January 2017
Available online xxxx

Keywords:
Ferritic steel
Inhibitor
Corrosion, sulphuric
Adsorption

ABSTRACT

The synergistic effect of the corrosion inhibition properties of 2-methoxy-4-formylphenol and sodium molybdenum oxide on the electrochemical property of 3CR12 ferritic stainless steel in 2M H_2SO_4 acid solution was assessed through coupon analysis, potentiodynamic polarization technique, IR spectroscopy and micro-analytical technique. Experimental data showed the combined admixture effectively inhibited the steel corrosion at the concentrations analyzed with a maximum inhibition efficiency of 94.47% and 89.71% from coupon analysis and potentiodynamic polarization due to the electrochemical action and inhibition of the steel by the ionized molecules of the inhibiting compound which influenced the mechanism of the redox reactions responsible to corrosion and surface deterioration. Results from corrosion thermodynamic calculations showed chemisorption adsorption mechanism. Infrared spectroscopic images exposed the functional groups of the molecules involved for the corrosion inhibition reaction. Micro-analytical images showed sharp contrast in surface morphology between the inhibited and corroded test specimens under study. Cracks, intergranular and pitting corrosion in addition to severe surface deterioration was observed in the uninhibited samples. Inhibitor adsorption fits the Langmuir isotherm model.

Introduction

Stainless steels are extensively applied industrially such as in desalination plants, petrochemical, construction, chemical processing, pharmaceutical, power generating plant, industrial cleaning, oil well acidizing and pickling process etc. because of their inherent stability, stable corrosion resistance and good mechanical properties. The excellent corrosion resistance is primarily as a result of the chemically produced oxide film which formed on its surface when exposed to an electrolyte. The film is the product of chemical interaction between iron substrate metal, chromium oxides formed and hydroxides at the metal-film interface [1]. The strength of the passive film is a product of the environment with which the stainless is exposed to and the alloy content. Corrosion deterioration of stainless steels is a major industrial problem with numerous investigators working to assess and control it. Most steels tends to be unstable in some conditions due to their inherent characteristics, reacting with the environments, forming a chemical compound in a more stable and lower energy state [2]. Damage due to corrosion is responsible for fluid leakages, structural weakness and eventual failure of stainless steels. This is responsible for the high cost for inspection/monitoring, repair/replacement and high cost of industrial end product, thus the need for cost effective corrosion control and inhibition measures [3]. 3CR12 ferritic stainless steel is the utility steel with the exceptional property high temperature and corrosion resistance as in other steel products coupled with their weldablity and formability. The steel is low priced with significant chromium content produced from the modification of grade 409 steel. It is resistant to mild corrosion and wet abrasion from strong acids and alkalis, and cracking resulted from chloride stress corrosion. The steel is employed in applications where aluminum, galvanized and carbon steels underperforms, however, its drawback is low resistance to crevice and pitting corrosion in chloride containing solutions.

One of the most cost proven and reliable means of preventing corrosion is through the consistent application of corrosion inhibitors. Inhibitors are generally applied to significantly reduce corrosion degradation on stainless steels. Chemicals of organic origin and constituents have been proven to be very effective corrosion inhibiting agents for a wide variety of steels in acidic medium. Use of organic compounds for corrosion inhibition has been

E-mail address: tolu.loto@gmail.com

http://dx.doi.org/10.1016/j.rinp.2017.01.042
2211-3797/

extensively studied and researched into [4,5]. Previous research has shown that organic compounds with one or more polar, heterocyclic functional groups and heteroatoms (N, O and S) with p-electrons are quite efficient in corrosion prevention [6]. The corrosion inhibition behavior of these organic compounds is the product of electrochemical interactions with metallic surfaces through chemisorption adsorption mechanism. The frequency of active centers of inhibitor adsorption, the degree of charge, the adsorption type, and the extent of exposed surface area covered of the compound control inhibition efficiency. The size, dimension and mass of the organic molecule also have significant impact of corrosion inhibition [7]. Molybdate based inhibitors are mildly effective in controlling anodic degradation of stainless steel in various aqueous neutral solutions [8–12]. They are non-toxic, environmentally sustainable corrosion inhibitors for the protection of soft-water cooling systems though there are few reports in literature on the protective properties of molybdate salts in acid solution. Their basic function in corrosion inhibition is adsorption onto metallic alloy exposed area to suppress the reactions associated with collapse of passive film [13,14]. Augustynski [15] suggested from his research that the corrosion inhibition property of the molybdate anions is probably due to reduction of Mo^{6+} to Mo^{4+} during the inhibition process. Current research has shown that one of the most important processes of inhibitor development is to improve the corrosion inhibition properties of existing inhibitors through synergistic effect in combination with others, thus this research aims to study the synergistic effect of 2-methoxy-4-formylphenol and sodium molybdenum oxide on the corrosion inhibition of 3CR12 ferritic stainless steel in dilute H_2SO_4 acid [16–19].

Experimental methods

Material

3CR12 ferritic stainless steel (FSS) with average elemental composition as shown below (Table 1) analysed at the Physical Metallurgy Laboratory, Department of Mechanical Engineering, College of Engineering, Covenant University, Ota, Ogun State, Nigeria. The steel is of a cylindrical shape with a diameter of 1.7 cm.

Inhibitor

Combined admixture of equal proportions of sodium molybdenum oxide and 2-methoxy-4-formylphenol, both as solid white precipitates (synthesized) were obtained from BOC Sciences, USA. Their structural formulae are shown in Fig. 1. Table 2 shows the chemical properties of the inhibiting compound. MPSB was prepared in concentrations of 6.982×10^{-6} M, 1.396×10^{-5} M, 2.095×10^{-5} M, 2.793×10^{-5} M, 3.491×10^{-5} M and 4.189×10^{-5} M in 200 mL of 2 M H_2SO_4 media.

Acid test solution

2 M H_2SO_4 acid solutions were prepared using analytical grade of the acid (98%) with deionized water.

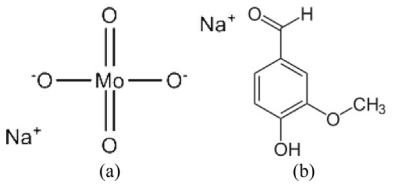

Fig. 1. Molecular structure of MPSB components (a) sodium molybdenum oxide, (b) 2-methoxy-4-formylphenol.

Table 2
Molecular properties of the MPSB inhibiting compound.

S/N	Compound	Molecular Formula	Molar Mass ($gmol^{-1}$)
1	Sodium molybdenum oxide	Na_2MoO_4	241.95
2	2-Methoxy-4-formylphenol	$C_8H_8O_3$	152.15

Sample preparation of ferritic stainless steels

The FSS and HCS samples were machined into seven (7) test pieces with mean length of 0.7 mm. The samples were further prepared metallographically using silicon carbide grit papers of 80, 300, 600 and 1000 grits before polishing to 6 µm with Pen Struers diamond paste. Each sample was cleansed with deionized water and propanone, and placed in a desiccator for coupon analysis and potentiodynamic polarization test according to ASTM G1 - 03(2011).

Coupon measurement

Ferritic steel coupons were measured before separate immersion in 200 mL of the corrosion test media for 240 h at of 30 °C. The samples were taking out separately from the electrolyte at 24 h meantime, cleansed with deionized water and propanone, dried and measured again according to ASTM G31-72(2004). Plots of corrosion rate values, ɤ (mm/y) and MPSB inhibition efficiency, η (%) against measured time T were outlined from the results obtained during the corrosion test period. Corrosion rate (ɤ) is determined as follows as [20].

$$ɤ = \left[\frac{87.6\omega}{DAT}\right] \quad (1)$$

ω is the mass loss in mg, D is the density in g/cm^3, A is the total surface area of the coupon in cm^2 and 87.6 is a constant. Inhibition efficiency (η) was determined from the expression below;

$$\eta = \left[\frac{\omega_1 - \omega_2}{\omega_1}\right] \times 100 \quad (2)$$

ω_1 and ω_2 are the mass loss at predetermined concentrations of MPSB. η was determined at the MPSB concentrations studied during the evaluation period. Surface coverage was evaluated from the expression [21,22]:

$$\theta = \left[1 - \frac{\omega_2}{\omega_1}\right] \quad (3)$$

Table 1
Elemental composition of FSS.

Element	C	Si	Mn	P	S	Cu	Ni	Cr	Fe
Composition (%)	0.050	0.182	1.830	0.12	0.017	0.102	1.3	13	82.80

Please cite this article in press as: Loto RT. Study of the synergistic effect of 2-methoxy-4-formylphenol and sodium molybdenum oxide on the corrosion inhibition of 3CR12 ferritic steel in dilute sulphuric acid. Results Phys (2017), http://dx.doi.org/10.1016/j.rinp.2017.01.042

where θ is the degree of MPSB compound, adsorbed per gram of the steel samples. ω_1 and ω_2 are the mass loss of each steel coupon at predetermined concentrations of MPSB in the acid media.

Potentiodynamic polarization technique

The polarization test was achieved with the cylindrical ferritic steel electrodes encased in acrylic resin mounts with exposed surface area of 254 and 132.7 mm^2. The electrodes were prepared with respect to ASTM G59-97(2014). Electrochemical studies were conducted at 30 °C using Digi-Ivy 2300 potentiostat and glass cell containing 200 mL of the corrosive test solution at predetermined concentrations of MPSB. Platinum rod was used as the counter electrode and silver chloride electrode (Ag/AgCl) as the reference electrode. Measurement was done from −1.5 V to +1.5 V at a scan rate of 0.0015 V/s according to ASTM G102-89(2015). Corrosion current density (j_{cr}) and corrosion potential (E_{cr}) were calculated from the Tafel outline of potential (V) versus current (log), (A cm^2). The corrosion rate (γ) and the inhibition efficiency (η_2, %) were evaluated from the expression below.

$$\gamma = \frac{0.00327 \times J_{corr} \times E_q}{D} \quad (4)$$

j_{cr} is the current density in μA/cm^2, D is the density in g/cm^3; E_{qw} is the sample equivalent weight in grams. 0.00327 is a constant for corrosion rate calculation in mm/y [23,24]. The inhibition efficiency (η_2, %) was calculated from corrosion rate values with the equation below;

$$\eta_2 = 1 - \left[\frac{\gamma_2}{\gamma_1}\right] \times 100 \quad (5)$$

γ_1 and γ_2 are the corrosion rates with and without MPSB inhibitor.

Optical microscopy characterization

Optical micrographs of the steel surface and morphology of the corroded and inhibited ferritic stainless steel samples was studied after weight-loss analysis with the aid of Omax trinocular optical metallurgical microscope at the Physical Metallurgical Laboratory, Covenant University, Ogun state, Nigeria.

Infrared spectroscopy

The MPSB compound in H_2SO_4 acid was exposed to specific range of infrared ray beams. The transmittance and reflectance of the infrared beams at various frequencies were decoded and transformed into an IR absorption plot consisting of spectra peaks. The spectral pattern was evaluated and equated according to IR absorption table to identify the functional groups involved in the corrosion inhibition reactions.

Result and discussion

Potentiodynamic polarization studies

Table 3 shows the data for influence of MPSB inhibitor on the corrosion polarization behaviour of FSS in 2M H_2SO_4. Fig. 2 shows the polarization plot obtained. Observation of Table 3 depicts the significant variation in corrosion rate and polarization resistance values for FSS samples at 0.25%–1.5% MPSB concentration in comparison to FSS sample at 0% MPSB. The corrosion rates for the inhibited FSS samples decreased consistently till 1.5% MPSB. This observation corresponds with the values obtained for polarization resistance (Table 3). At 0.25% MPSB the inhibition efficiency is at the lowest (81.13%) but increases with increase in MPSB concentration to 89.71% at 1.5% MPSB. The results show that MPSB

Table 3
Polarization results for FSS in 2M H_2SO_4 at 0%–1.5% MPSB.

Sample	MPSB Conc. (M)	MPSB Conc. (%)	Corrosion rate (mm/y)	Inhibition efficiency (%)	Corrosion current (A)	Corrosion current density (A/cm^2)	Corrosion potential (V)	Polarization resistance, R_p (Ω)	Cathodic potential, B_c (V)	Anodic potential, B_a (V)
A	0	0	21.03	0	4.33E−03	1.91E−03	−0.376	7.28	−1.044	3.10E−02
B	6.98E−06	0.25	3.97	81.13	8.18E−04	3.60E−04	−0.313	36.30	−8.804	3.00E−02
C	1.40E−05	0.5	3.65	82.64	7.52E−04	3.31E−04	−0.292	45.00	−8.156	3.42E−02
D	2.09E−05	0.75	3.74	82.22	7.71E−04	3.39E−04	−0.294	38.18	−8.636	2.97E−02
E	2.79E−05	1	3.30	84.30	6.81E−04	3.00E−04	−0.270	44.95	−7.705	3.09E−02
F	3.49E−05	1.25	2.52	88.01	5.20E−04	2.29E−04	−0.253	40.61	−4.891	2.13E−02
G	4.19E−05	1.5	2.16	89.71	4.46E−04	1.96E−04	−0.283	45.99	−7.002	2.07E−02

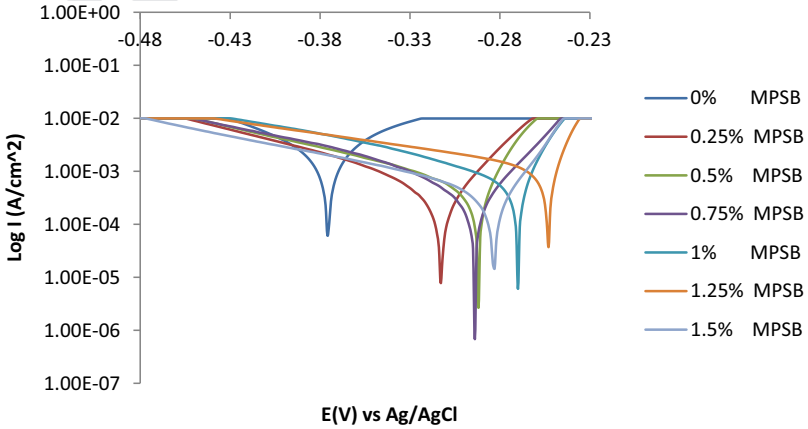

Fig. 2. Anodic and cathodic polarization plots for FSS in 2M H_2SO_4 at 0%–1.5% MPSB.

Please cite this article in press as: Loto RT. Study of the synergistic effect of 2-methoxy-4-formylphenol and sodium molybdenum oxide on the corrosion inhibition of 3CR12 ferritic steel in dilute sulphuric acid. Results Phys (2017), http://dx.doi.org/10.1016/j.rinp.2017.01.042

Table 4
Data for 3CR12 ferritic steel in 2M H_2SO_4 at predetermined concentrations of MPSB from weight loss analysis.

FSS Samples	Weight Loss (g)	Corrosion Rate (mm/yr)	MPSB Inhibition Efficiency (%)	MPSB Concentration (%)	MPSB Concentration (Molarity)
A	11.264	0.060	0	0	0
B	1.617	0.009	85.65	0.13	6.9819E−06
C	1.479	0.008	86.87	0.25	1.3964E−05
D	2.165	0.012	80.78	0.38	2.0946E−05
E	0.711	0.004	93.68	0.50	2.7928E−05
F	0.367	0.002	96.74	0.63	3.4909E−05
G	0.623	0.003	94.47	0.75	4.1891E−05

effectively inhibits the corrosion of FSS in H_2SO_4 at the concentrations studied. The corrosion current also decreased significantly with increment in concentration of MPSB. The inhibition efficiency of MPSB is dependent to a minimal degree on the values of its concentration in the acid media. This is due to the presence of an effective MPSB film which prevents corrosion by limiting the diffusion of sulphate anions (SO_4^{2-}) to the metal surface, as well as inhibiting the electrolytic transport of metallic cations. It is also suggested that MPSB modifies the corrosive environment, significantly weakening the oxidizing strength of the corrosive media [25,26].

The anodic/cathodic polarization plots in Fig. 2 shows active and anodic-passivation polarization behavior with and without MPSB compound. The plot for 0% MPSB shows corrosion potential of −0.376 V which corresponds to values of active corrosion reactions and deterioration of the FSS. The polarization plots for FSS samples with varying degree of MPSB concentration occurred at corrosion potentials (−0.313V–−0.283 V) which correspond to passivation potentials. Even though similar electrochemical behavior was observed, the corrosion potential shifts entirely towards anodic values suggesting that the inhibition mechanism is probably through suppression of the anodic oxidation reactions responsible for FSS dissolution ($Fe \rightarrow Fe^{2+} + 2e^-$) [27]. This phenomenon is further supported from results obtained for polarization resistance on Table 3 where the values increased from 36.39 Ω–45.99 Ω. The molybdate ion is an anodic corrosion inhibitor and the synergistic effect of 2-methoxy-4-formylphenol component of MPSB does not change its inhibition property [17]. Previous research has shown that the 2-methoxy-4-formylphenol component of MPSB is a mixed type inhibitor with strong influence on cathodic reactions. Its physicochemical characteristics are due to the composition of its functional groups (aldehyde, hydroxyl, and ether) and their electrochemical property [28]. This property is through the charge of the carbonyl group and the astringency of any α-hydrogen within their structure. The hydroxyl groups within the compound are polarized in the electrolyte to enable the O_2 atom release electron. The hydroxyl group causes electrostatic attraction with the metal [29]. The compound accumulates a passive hydrophobic covering of inhibitor molecules adsorbed onto the alloy, which prevents the dissolution of the metal within the aqueous solution.

The precipitation Fe^{2+}-MPSB on the anodic area of the steel controls the anodic reaction. The reduction reaction is under the influence of $Zn(OH)_2$ formation on the cathodic areas of the metal surface. The anodic and cathodic Tafel slopes were slightly influenced by changes in MPSB concentration suggesting that changes to the redox reactions relating to the mechanism of inhibition is through decrease in the surface area of FSS for corrosion process [30]. The optimal change in corrosion potential in H_2SO_4 is 123 mV in the anodic direction, thus MPSB is an anodic type inhibitor [29,31]. The molybdate ion component of MPSB has a higher radius than the sulfate anion, thus a higher specific adsorption [32]. It absorbs onto the steel surface and is reduced (Mo^{6+} reduces to Mo^{4+}, MoO_2 is formed) according to the reaction in Eq. (6) [14]. The reaction of H^+ with O^{2-} simultaneously results in the dilution of local solution acidity causing a less oxidizing solution. The molybdate ion scavenges the dissolved oxygen, stifles the anode reaction and supports the passivation of the metal surface.

$$MoO_4^{2-} + 4H^+ + 2e^- = MoO_2 + 2H_2O \quad (6)$$

Coupon measurements

Calculated results obtained for weight loss ($\tilde{\omega}$), corrosion rate ($\curlyvee$) and percentage inhibition efficiency ($\wp$) for the interaction of MPSB inhibiting compound on FSS in H_2SO_4 solutions are presented in Table 4. Figs. 3 and 4 show the plot of corrosion rate and MPSB inhibition efficiency versus exposure time in the acid media. MPSB had a strongly influenced the reduction-oxidation corrosion reactions responsible for FSS degradation. MPSB being an anodic inhibitor as discussed previously, its inhibition mode is through adsorption whereby it precipitates on the reactive sites of the steel surface. The release of FSS cations into the acid solution through the electrochemical action of sulphate ions was significantly minimized. Observation of Table 4 and Fig. 3 show the significant variation in corrosion rate values between the uninhibited FSS sample and samples inhibited by MPSB similar in trend to observation from potentiodynamic polarization test. The corrosion rate for FSS at 0% MPSB concentration decreases steadily

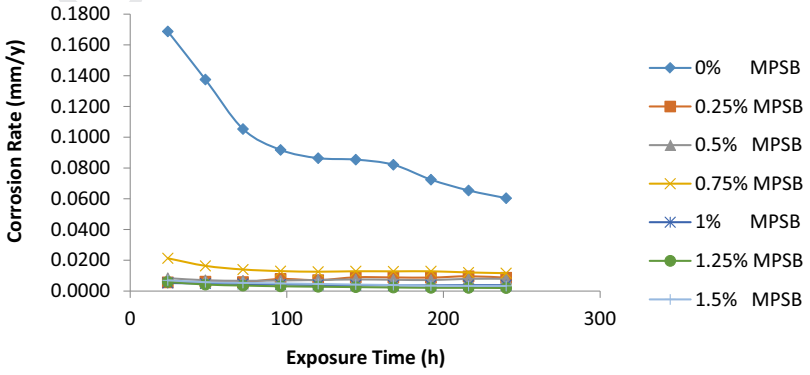

Fig. 3. Plot of corrosion rate versus exposure time for 3CR12 ferritic steel in 2M H_2SO_4 at 0–1.5%MPSB.

Please cite this article in press as: Loto RT. Study of the synergistic effect of 2-methoxy-4-formylphenol and sodium molybdenum oxide on the corrosion inhibition of 3CR12 ferritic steel in dilute sulphuric acid. Results Phys (2017), http://dx.doi.org/10.1016/j.rinp.2017.01.042

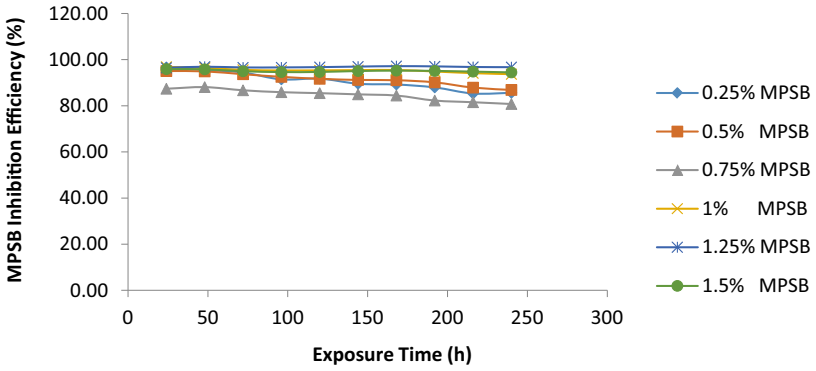

Fig. 4. Plot of inhibition versus exposure time for 3CR12 ferritic steel in 2M H_2SO_4 at 0–1.5%MPSB.

till the end of the exposure period. Addition of predetermined MPSB concentration (0.25% MPSB–1.5% MPSB) caused the corrosion rate values to decline sharply. The values were generally the same throughout the experiment.

The strong absorption of MPSB ionized molecules onto FSS surface is due to the synergistic effect of the sodium molybdenum oxide and 2-methoxy-4-formylphenol components of MPSB compound. Adsorption by 2-methoxy-4-formylphenol on the cathodic and anodic area takes place through the π-electrons of molecular bond in the rings and lone pair of electrons from the hetero atoms present, which suppresses the anodic oxidation of the steel. This component of MPSB consists of electron rich heteroatoms involved in Lewis acid-base interaction with the steel [33]. They act through formation of a protective film over the exposed metal surface. The film adsorbs through chemical reaction mechanism onto the steel preventing the oxidation reaction of corrosive ions with the steel [34]. The molybdate ions of sodium molybdenum oxide adsorb on the surface of the steel and form a complex with the ferrous (Fe^{+2}) ions. The complex though unstable, oxidizes in the presence of dissolved oxygen to give insoluble ferric (Fe^{+3}) ions which forms an insoluble protective barrier of ferric molybdate [35].

Adsorption isotherm

Adsorption of MPSB ionized molecules on FSS surface occurs at the metal ion/solution interface and is subject to the intermolecular/electrostatic forces at the interface. The ionization potential, metallic surface charge/properties, electronic properties, degree of ionic adsorption and the electrochemical potential strongly influence the mechanism and type of adsorption [36]. Further studies of the adsorption characteristics of MPSB compound were done to understand the interaction mechanism between the MPSB and FSS ions. Langmuir adsorption isotherm model amongst other isotherms gave the best fit for the results obtained for MPSB on FSS in H_2SO_4 acid solution.

The conventional depiction of the Langmuir isotherm is shown in Eq. (7) below;

$$\theta = \left[\frac{K_{ads}C}{1 + K_{ads}C}\right] \quad (7)$$

θ is the degree of surface coverage of the inhibitor on the alloy surface, C is MPSB concentration in H_2SO_4 acid media, and K_{ads} is the equilibrium constant of the adsorption process. The plots of $\frac{C}{\theta}$ versus the MPSB concentration were linear (Fig. 5) justifying the Langmuir adsorption.

According to Langmuir, MPSB cations adsorb at specific reaction sites at the metal/ solution boundary causing the slight deviation of slope from unity in Fig. 6(a) and (b) [37,38]. Increase in MPSB concentration causes changes in the energy and force of interaction with water molecules as MPSB molecules increasingly adsorb on the steel.

Thermodynamics of the corrosion inhibition mechanism

Results of Gibbs free energy (ΔG^o_{ads}) for MPSB adsorption on FSS (Table 5) was evaluated from Eq. (8).

$$\Delta G_{ads} = -2.303RT\log[55.5K_{ads}] \quad (8)$$

where 55.5 is the molar concentration of water in the solution, R is the universal gas constant, T is the absolute temperature and K_{ads} is the equilibrium constant of adsorption for MPSB. K_{ads} is related to surface coverage (θ) from Eq. (8).

The heterogeneous characteristics of FSS morphology cause the changes in ΔG^o_{ads} of adsorption for MPSB with changes in surface

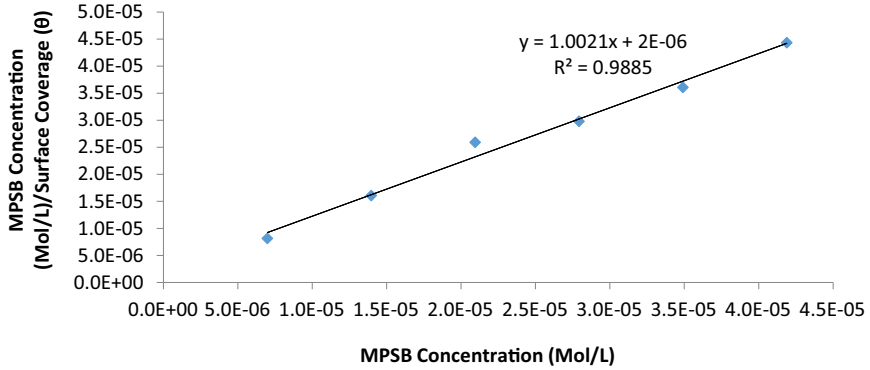

Fig. 5. Plot of $\frac{C}{\theta}$ versus MPSB concentration (C) in 2M H_2SO_4.

Please cite this article in press as: Loto RT. Study of the synergistic effect of 2-methoxy-4-formylphenol and sodium molybdenum oxide on the corrosion inhibition of 3CR12 ferritic steel in dilute sulphuric acid. Results Phys (2017), http://dx.doi.org/10.1016/j.rinp.2017.01.042

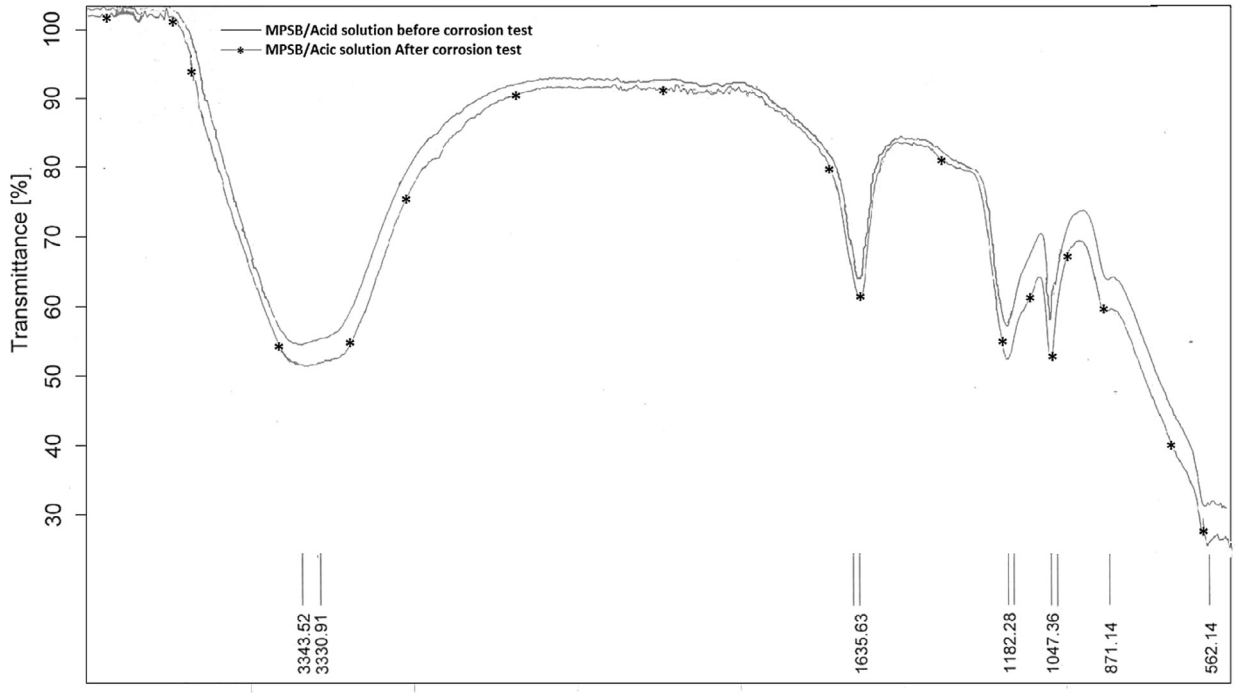

Fig. 6. IR spectra of MPSB compound in 2M H_2SO_4 acid before and after FSS corrosion.

Table 5
Data for Gibbs free energy, surface coverage and equilibrium constant of adsorption for 0–1.5% MPSB in 2 M H_2SO_4.

Samples	MPSB concentration (%)	Surface coverage (θ)	Equilibrium constant of adsorption (K)	Gibbs free energy, ΔG (Kjmol^{-1})
A	0	0	0	0
B	0.25	0.856	854698.9	−43.80
C	0.5	0.869	473734.0	−42.34
D	0.75	0.808	200697.9	−40.21
E	1	0.937	531040.7	−42.62
F	1.25	0.967	850030.1	−43.79
G	1.5	0.945	407640.1	−41.96

coverage values [39–41]. This relationship is responsible for the differences in adsorption energies presented in the Table 5. The negative values of ΔG^o_{ads} show the adsorption mechanism is spontaneous [42]. Values of ΔG^o_{ads} around −40 kJmol^{-1} depict chemisorption adsorption reactions. Reactions at this value involve charge sharing or transfer between the inhibitor cations and the valence electrons of the steel forming a co-ordinate covalent bond. The highest ΔG^o_{ads} value in H_2SO_4 is −43.80 kJ mol^{-1} at 0.25% MPSB while the lowest is −41.96 kJ mol^{-1} at 1% MPSB.

IR spectroscopy

The IR spectra of 2M H_2SO_4/MPSB solution before and after the corrosion tests are shown in Fig. 6. Observation of the spectra peaks shows that the test solution had almost similar peaks; however, the intensities decreased/increased at some spectra peaks after the corrosion test due to the reaction of MPSB with FSS and acid to form chemical complexes. The spectra peaks of 3343.52, 1635.63, 1182.28, 1047.36, 871.14 and 562.14 cm^{-1} before the corrosion test generally corresponds to O–H stretch, H–bonded (alcohols, phenols), N–H stretch (primary, secondary amines, amides) and C–H "oop" (aromatics) [43]. The amines and hydroxides functional groups have been shown from previous research to be good corrosion inhibitors [44–46]. The spectra peak after corrosion test presents the same molecular functional groups at near similar peak values of 3330.91, 1635.77, 1181.46, 1047.21 and 873.59 cm^{-1}.

Comparison of the spectra before and after the corrosion test clearly reveals the decrease in transmittance indicators for the functional groups earlier mentioned, they involved in the electrochemical reaction resulting in inhibition of the steel through adsorption. The intensity of the peaks of 1181.46, 1047.21 and 873.59 cm^{-1} after the corrosion test significantly decreased due to the strong reaction of the inhibitor molecules at those peaks with the metal through chemical reaction mechanism. The groups instigates the formation of stable chemical precipitates between the substrate metal composition of FSS and MPSB compound. The complexes tend to suppress the corrosion reaction mechanisms inhibiting FSS surface [47].

Optical microscopy analysis

Optical micrographs of FSS samples before and after the corrosion test are shown from Figs. 7a–9c. The micrographs of FSS samples before the test at mag. x4, x40 & x100 are shown in Fig. 7(a)–(c). The micrographs depict the sample surface after undergoing metallographic procedures and clearly reveal the serrated edges after machining. Fig. 8(a) shows the micrograph of the uninhibited FSS after the corrosion test. Morphological deterioration and of the surface topography can be observed due to the redox electrochemical reactions of corrosive ions present in the acid media. The ions cause the release of valence electrons and diffusion of Fe^{2+} cations into the acid solution. Zooming in on Fig. 8(a), Fig. 8(b) clearly

Please cite this article in press as: Loto RT. Study of the synergistic effect of 2-methoxy-4-formylphenol and sodium molybdenum oxide on the corrosion inhibition of 3CR12 ferritic steel in dilute sulphuric acid. Results Phys (2017), http://dx.doi.org/10.1016/j.rinp.2017.01.042

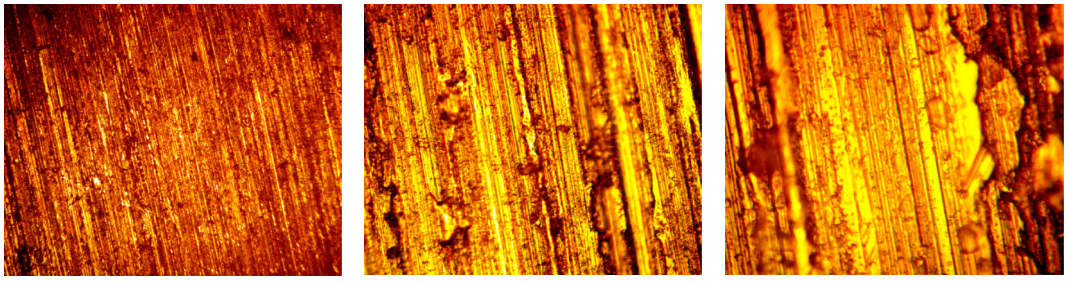

Fig. 7. Micrographs of FSS before corrosion test (a) mag. x4, (b) mag. x40 and (c) mag. x100.

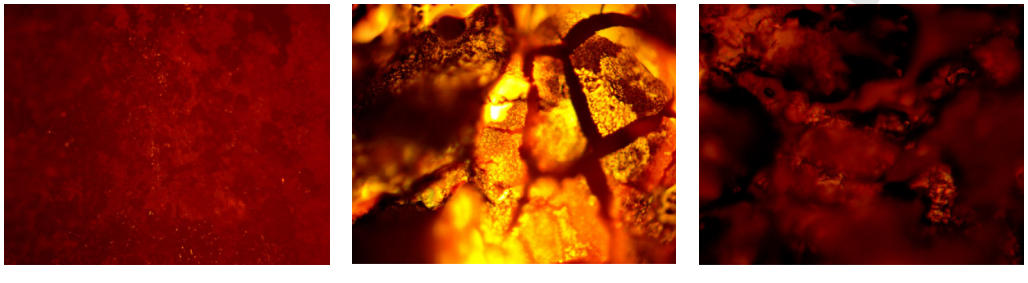

Fig. 8. Micrographs of FSS after corrosion test without MPSB compound (a) mag. x4, (b) mag. x40 and (c) mag. x100.

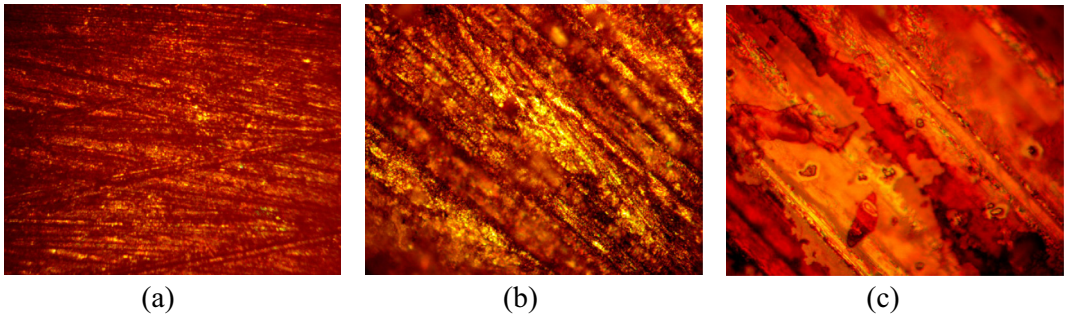

Fig. 9. Micrographs of FSS after corrosion test with MPSB compound (a) mag. x4, (b) mag. x40 and (c) mag. x100.

identifies some specific areas of morphological deterioration especially at the grain boundary. This clearly shows that intergranular corrosion is partly responsible for the corrosion of FSS, micro-pits due to pitting can also be observed though less visible. These observations [Fig. 8(a)–(c)] show that FSS steel cannot be applied in high sulphate containing industrial environments due to rapid deterioration. The micrographs in Fig. 9(a)–(c) contrast the images in Fig. 8(a)–(c); Fig. 9(a)–(d) show the images of FSS samples from the electrolyte with MPSB compound after coupon analysis. The images reveal a slightly worn surface in comparison to the untested specimens in Fig. 7(a)–(c). MPSB compound effectively protected the FSS samples and the images conforms the results obtained from weight loss and potentiodynamic polarization. The combined action of molybdate ions and heteroatoms of the phenolic aldehydes adsorbs onto the steel, reacting with the surface through chemical reaction mechanism.

Conclusion

MPSB performed effectively in the acid media inhibiting the corrosion of 3CR12 ferritic stainless steel. The corrosion protection efficiency values of the compound deviated slightly at the concentrations evaluated as a result of the inhibition reaction of the molecular functional groups and heteroatoms of the compounds which influenced the mechanism of the redox electrochemical reactions and protecting the steel from corrosion. The compound was determined to be anodic type inhibitor. Thermodynamic calculations confirm strong chemisorption reaction mechanism and the adsorption aligned with the Langmuir adsorption isotherm. Infrared spectra images confirmed the adsorption of primary and secondary amines and hydroxides onto the steel.

Acknowledgement

The authors acknowledge the Department of Mechanical Engineering, Covenant University, Ota, Ogun State, Nigeria for the provision of research facilities for this work.

References

[1] Marcus P, Olefjord IA. Round robin on combined electrochemical and AES/ESCA characterization of the passive films on FeCr and FeCrMo alloys. Corros Sci 1988;28(6):589–602.

Please cite this article in press as: Loto RT. Study of the synergistic effect of 2-methoxy-4-formylphenol and sodium molybdenum oxide on the corrosion inhibition of 3CR12 ferritic steel in dilute sulphuric acid. Results Phys (2017), http://dx.doi.org/10.1016/j.rinp.2017.01.042

[2] Ayo SA. Synergistic inhibition of potassium chromate and sodium nitrite on mild steel in chloride and sulphide media. Leonardo Electron J Practices Technol 2007;11:143–54.
[3] Ashish KS, Quraishi MA. Effect of 2, 20 benzothiazolyl disulfide on the corrosion of mild steel in acid media. Corros Sci 2009;51(11):2752–60.
[4] Fekry AM, Mohamed RR. Acetyl thiourea chitosan as an ecofriendly inhibitor for mild steel in sulfuric acid medium. Electrochim Acta 2010;55(6):1933–9.
[5] Heakal FE, Fekry AM. Experimental and theoretical study of uracil and adenine inhibitors in Sn-Ag alloy/nitric acid corroding system. J Electrochem Soc 2008;155:C534–42.
[6] Fekry AM, Ameer MA. Corrosion inhibition of mild steel in acidic media using newly synthesized heterocyclic organic molecules. Int J Hydrogen Energy 2010;35(14):7641–51.
[7] Munoz LD, Bergel A, Fe'ron D, Basseguy R. Hydrogen production by electrolysis of a phosphate solution on a stainless steel cathode. Int J Hydrogen Energy 2010;35(16):8561–8.
[8] Gong X, Li Y, Peng K, Xie X. Electrochemical behavior of molybdate inhibitor in tap water. Corros Sci Prot Technol 2001;13(4):208–10.
[9] Saji VS, Shilbi SMA. Mitigating corrosion of mild steel by sodium tungstate based inhibitors in neutral aqueous medium. Trans SAEST 2002;37(1):17–24.
[10] Mu G, Li X, Qu Q, Zhou J. Molybdate and tungstate as corrosion inhibitors for cold rolling steel in hydrochloric acid solution. Corros Sci 2006;48(2):445–59.
[11] Cansever N, Cakir AF, Urgen M. Inhibition of stress corrosion cracking of AISI 304 stainless steel by molybdate ions at elevated temperatures under salt crust. Corros Sci 1999;41(7):1289–303.
[12] Virtanen S, Surber B, Nylund P. Influence of MoO_4^{2-} anion in the electrolyte on passivity breakdown of iron. Corros Sci 2001;43(6):1165–77.
[13] Szklarska – Smialowska Z. Pitting and crevice corrosion; Nace, Houston; 2005. p. 590.
[14] Ilevbare GO, Burstein GT. The inhibition of pitting corrosion of stainless steels by chromate and molybdate ions. Corros Sci 2003;45(7):1545–69.
[15] Augustynski J. In: Frankenthal RP, Kruger J, editors. Passivity of Metals. Remington, New Jersey: Electrochemical Society; 1978. p. 989.
[16] Bentley AJ, Earwaker LG, Farr JPG, Seeney AM. A technique for the in situ elemental analysis of electrode surfaces. Surf Tech 1984;23(1):99–103.
[17] Farr JPG, Saremi M. Molybdate in aqueous corrosion inhibition I: effects of molybdate on the potentiodynamic behaviour of steel and some other metals. Surf Tech 1983;19(2):137–44.
[18] Mustafa CM, Dulal SMSI. Molybdate and nitrite as corrosion inhibitors for copper-coupled steel in simulated cooling water. Corrosion 1996;52(1):16–22.
[19] Alexander DB, Moccari AA. Evaluation of corrosion inhibitors for component cooling water systems. Corrosion 1993;49(11):921–8.
[20] Venkatesan P, Anand B, Matheswaran P. Influence of formazan derivatives on corrosion inhibition of mild steel in hydrochloric acid medium. E-J Chem 2009;6(S1):S438–44.
[21] Abbasova VM, Abd El-Lateefa HM, Aliyevaa LI, Qasimova EE, Ismayilova IT, Khalaf MM. A study of the corrosion inhibition of mild steel C1018 in CO_2-saturated brine using some novel surfactants based on corn oil. Egypt J Pet 2013;4(22):451–70.
[22] Sethi T, Chaturvedi A, Mathur RK. Corrosion inhibitory effects of some Schiff's bases on mild steel in acid media. J Chilean Chem Soc 2007;3(52):1206–13.
[23] Ahmad K. Principles of corrosion engineering and corrosion control. Oxford, UK: Butterworth-Heinemann; 2006.
[24] Choi Y, Nesic S, Ling S. Effect of H_2S on the CO_2 corrosion of carbon steel in acidic solutions. Electrochim Acta 2011;56:1752–60.
[25] Strainick MA. Corrosion inhibition of metals by molybdate. Part I. mild steel. Corrosion 1984;40(6):296–302.
[26] Husain KH, Jarman R. The inhibition effect of sodium molybdate on the initiation of corrosion fatigue of 1020 mild steel in aqueous solution. Desalination 1994;99(1):113–8.
[27] Finšgar M, Jackson J. Application of corrosion inhibitors for steels in acidic media for the oil and gas industry: a review. Corros Sci 2014;86:17–41.
[28] Loto RT. Electrochemical analysis of the corrosion inhibition properties of 4-hydroxy-3-methoxybenzaldehyde on low carbon steel in dilute acid media. Cogent Eng 2016;3:1242107.
[29] Dieter L. Corrosion and surface chemistry of metals. EPFL Press; 2007. p. 67.
[30] Philip JYN, Buchweshaija J, Mwakalesi A. Corrosion Inhibition of amino pentadecylphenols (APPs) derived from cashew nut shell liquid on mild steel in acidic medium. Mater Sci Appl 2016;7:396–402.
[31] Susai RS, Mary R, Noreen A, Ramaraj R. Synergistic corrosion inhibition by the sodium dodecylsulphate–Zn^{2+} system. Corros Sci 2002;44(10):2243–52.
[32] Sahin M, Bilgiç S, Yılmaz H. The inhibition effects of some cyclic nitrogen compounds on the corrosion of the steel in NaCl mediums. Appl Surf Sci 2002;195(104):1–7.
[33] Refaey SAM, Abd El-Rehim SS, Taha F, Saleh MB, Ahmed RA. Inhibition of chloride localized corrosion of mild steel by PO_4^{3-}, CrO_4^{2-}, MoO_4^{2-}, and NO_2^- anions. Appl Surf Sci 2000;158(3–4):190–6.
[34] James OO, Ajanaku KO, Ogunniran KO, Ajani OO, Siyanbola TO, John MO. Adsorption behaviour of pyrazolo [3, 4-b] pyridine on corrosion of stainless steel in HCl solutions. Trends Appl Sci Res 2011;6(8):910–7.
[35] Felicia RS, Santhanalakshmi S, Wilson SJ, John AA, Susai R. Synergistic effect of succinic acid and Zn^{2+} in controlling corrosion of carbon steel. Bull Electrochem 2004;20(12):561–5.
[36] Lawrence JK. Metals handbook, corrosion, 9th ed., vol. 13: ASM; 1987. p. 494–5.
[37] Loto RT, Loto CA. Corrosion inhibition properties of the combined admixture of thiocarbanilide and hexadecyltrimethylammoniumbromide on mild steel in dilute acid solutions. Cogent Chem 2016;2(1). http://dx.doi.org/10.1080/23312009.2016.1268377.
[38] Abiola OK. Adsorption of 3-(4-amino-2-methyl-5-pyrimidyl methyl)-4-methyl thiazolium chloride on mild steel. Corros Sci 2006;48:3078–90.
[39] Bockris JOM. Modern electrochemistry, vol. 2. London: Macdonald Ltd.; 1970. p. 772.
[40] Damaskin BB, Frumkin AN. Adsorption of molecules on electrodes. London: Wiley-Interscience; 1971. p. 36.
[41] Li XH, Deng SD, Fu H, Mu GN. Inhibition by tween-85 of the corrosion of cold rolled steel in 1.0 M hydrochloric acid solution. J Appl Electrochem 2009;39:1125–35.
[42] Lowmunkhong P, Ungtharatak D, Sutthivaiyakit P. Tryptamine as a corrosion inhibitor of mild steel in hydrochloric acid solution. Corros Sci 2010;52:30–6.
[43] Table of Characteristic IR Absorptions.http://orgchem.colorado.edu/Spectroscopy/specttutor /irchart.pdf. [Accessed: 12/01/2017].
[44] Benali O, Benmehdi H, Hasnaoui O, Selles C, Salghi R. Green corrosion inhibitor: inhibitive action of tannin extract of Chamaerops humilis plant for the corrosion of mild steel in 0.5 M H_2SO_4. J Mater Environ Sci 2013;4 (1):127–38.
[45] Fouda AS, Mostafa HA, El-Taib F, Elewady GY. Synergistic influence of iodide ions on the inhibition of corrosion of C-steel in sulphuric acid by some aliphatic amines. Corros Sci 2005;47(8):1988–2004.
[46] Gao G, Liang CH, Wang H. Synthesis of tertiary amines and their inhibitive performance on carbon steel corrosion. Corros Sci 2007;49(4):1833–46.
[47] Zheludkevich ML, Poznyak SK, Rodrigues LM, Raps D, Hack T, Dick LF, Nunes T, Ferreira MGS. Active protection coatings with layered double hydroxide nanocontainers of corrosion inhibitor. Corros Sci 2010;52(2):602–11.

Please cite this article in press as: Loto RT. Study of the synergistic effect of 2-methoxy-4-formylphenol and sodium molybdenum oxide on the corrosion inhibition of 3CR12 ferritic steel in dilute sulphuric acid. Results Phys (2017), http://dx.doi.org/10.1016/j.rinp.2017.01.042